Braz J Phys (2014) 44:368–379
DOI 10.1007/s13538-014-0212-z

NUCLEAR PHYSICS

Ring-Like and Jet-Like Events in Ultra High-Energy Interactions—an Analysis in Terms of Multifractal Parameters

Dipak Ghosh · Argha Deb · Mitali Mondal · Aparna Dhar (Mitra) · Soma Biswas (Ghosh)

Received: 20 June 2013 / Published online: 4 June 2014

Abstract Ring-like and jet-like events produced in ^{16}O-AgBr interactions at 60 AGeV are analyzed in terms of multifractal G-moment method and factorial moment method in both η space and ϕ space for emitted pions. Further, the Levy indices and multifractal specific heat c have been calculated. The results clearly indicate that μ and c both are different in ring-like and jet-like events depicting different mechanism in the production process.

Keywords Relativistic heavy ion collision · Fractal structure · Ring-like and jet-like events · Degree of multifractality · Multifractal specific heat

1 Introduction

Analysis of azimuthal distribution of pions in case of ultra relativistic heavy ion collisions reveals two different classes of substructures, which are referred to as ring-like and jet-like structures. These structures are also referred to as tower and wall structures [1]. Ring-like structures are occurrences where many pions are produced in narrow regions along the pseudorapidity (η) axis, which are at the same time diluted over whole azimuth (φ) like the spokes of a wheel as shown in Fig. 1a. If the jet-emitting gluons are small, then it is more likely that several jets, each restricted to narrow intervals in both η and φ directions, will be formed, thereby resulting in jet structures in the distributions of final-state hadrons [2] as shown in Fig. 1b.

The origin of ring-like events is still unknown. Several theories have come up in this regard. It is suggested that, similar to electromagnetic interactions, strong interactions might induce coherent collective effects in hadronic matter which results in the so-called ring-like events. The analogue to Cherenkov photons would be Cherenkov gluons emitted by a parton (quark) entering a hadronic medium [3–6]. An alternative approach, however, may be to consider the formation of a Mach shock wave travelling through the nuclear medium that may also result in the preferential emission of final-state hadrons [7, 8]. The complete and consistent theory of ring-like and jet-like structures is yet to be formulated.

The study of the multiplicity fluctuation in particle production at high energy has revealed self-similar properties conjectured by Bialas and Peschansky [9, 10] who called the phenomenon, the intermittency. The self-similar nature of the vortices directly implies a connection between intermittency and fractality. Various experimental and theoretical activities have been carried out in the past in search of scale invariance and fractality in nuclear collisions at high energy [9, 11, 12].

The word fractal was first coined by Mandelbrot [13], who discovered that there is a fractal face to the geometry of nature. Mandelbrot, the pioneer, opened a new window, namely, the fractal geometry for looking into the world of apparent irregularities. The most notable property of fractals is their dimension. Hwa introduced the multifractal moment G_q, to study the multifractality and self-similarity in multiparticle production. The basic characteristic of multifractality is the difference in scaling properties in different regions of the system.

In order to suppress the statistical contribution, a modified form of G moments in terms of the step function was suggested by Hwa and Pan [14] which can act as a filter for low multiplicity events. The method has been applied to understand multifractality in lepton, hadron, and nuclear collisions [15–19].

D. Ghosh · A. Deb · A. Dhar (Mitra) · S. Biswas (Ghosh)
Nuclear and Particle Physics Research Centre, Department of Physics, Jadavpur University, Kolkata 700032, India

M. Mondal (✉)
S. A. Jaipuria College, Kolkata 700005, India
e-mail: mitalimon@gmail.com

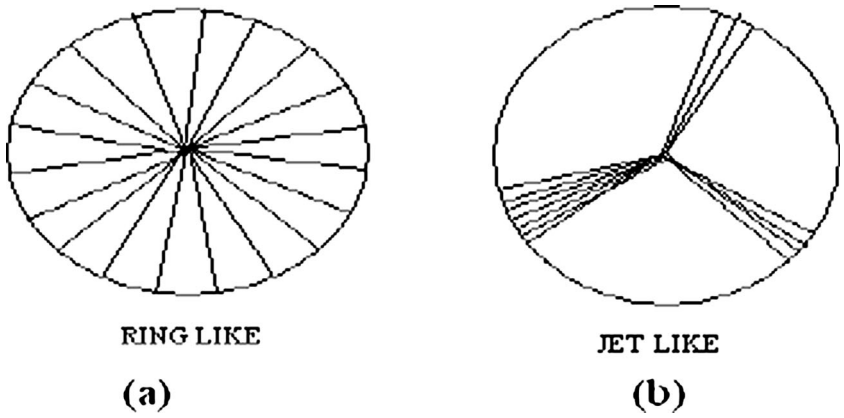

Fig. 1 Schematic representation of the two extreme azimuthal structures—**a** ring and **b** jet like

It is known, in particular, that the multifractality can be considered from a thermodynamic point of view [20–22]. This interpretation is usually used to study the phase transition like phenomena in the intermittent data [21, 23, 24]. On the other hand, some simple thermodynamic approximations could be applicable to the multiparticle production. Bershadkii [25] has pointed out that in many important thermodynamical cases, the specific heats of solids and gases are constant, independent of temperature over a certain temperature interval [26]. The entropy $f(q)$ in this case can be approximated by the following relation $f(q)=a-c\ln q$, where a is a constant and c is constant specific heat (CSH). Using the constant a, one can get the generalized dimension D_q from CSH approximation as $D_q = (a-c) + c\frac{\ln q}{q-1}$.

If one plots D_q vs $\ln q/(q-1)$, the slope of the graph will give the value of specific heat.

It was concluded in [27] that all the data exhibit multifractal Bernoulli fluctuations. It was noticed that the values of multifractal specific heat obtained for very heavy and moderately heavy ions seemed to be universal (≈1/4), whereas, for relatively "light" heavy ions, no such universality was found.

During 2nd-order phase transition, the system becomes scale invariant and the anomalous fractal dimension becomes equal to each other [28] exhibiting a monofractal behavior. However, in self-similar cascades (partonic and/or hadronic), the anomalous fractal dimensions are sensitive to the details of the vertex describing the cascade, and thus, the anomalous dimensions show (linear) dependence on q, and the system behaves as a multifractal one.

For self-similar cascade mechanism, the probability density distribution of the pions may be obtained by using the Levy stable law, i.e., characterized by the Levy stability index μ, considered to be a measure of degree of multifractality corresponding to the physically allowed limit. Within the region of stability, $0\leq\mu\leq2$, μ has a continuous spectrum [29]. The two bound axis of the Levy index correspond to the degree of fluctuation in particle production. $\mu=2$ corresponding to the minimum fluctuation from self-similar branching processes, and $\mu=0$ corresponding to maximum fluctuation which characterizes the interacting system as monofractal [24, 30]. According to Ref. [29], when $\mu<1$, there is a thermal phase transition (interspersed in the cascading process if $\mu>0$). On the other hand, if $\mu>1$, there is a nonthermal phase transition during the cascading process.

In this paper, we have presented an investigation on fractal properties and associated possible 2nd-order phase transition [31] of the ring-like and jet-like substructures of the data on pions coming from ^{16}O-AgBr interactions at 60 AGeV using G-moment method [32–35] and factorial moment method [9, 10]. The analysis has been performed in one-dimensional pseudorapidity and azimuthal angle space. The values of the generalized factorial dimension D_q have been evaluated from each corresponding method using adequate mathematical formula. Also, the values of the multifractal specific heat c has been calculated from the values of D_q obtained from the G-moment and factorial moment methods. The Levy indices are calculated for all the cases to investigate the nature of phase transition.

2 Experimental Details

The data used in the present investigation have been obtained from sets of Illford G5 nuclear emulsion stacks exposed to a ^{16}O-beam with incident energy 60 AGeV at the CERN SPS. The stack of rectangular nuclear emulsion plates were exposed to parallel projectile beam from the accelerator. The beam entrance direction in the plates was marked by arrow. It is done so that one can easily identify the primary beam tracks (parallel to each other) and the direction of their movement through the emulsion medium. An event initiated by such a primary projectile beam is considered to be a real primary event.

A Leitz Metaloplan microscope with a 10× objective and 10× ocular lens provided with a semiautomatic scanning stage was used to scan the plates. The final measurements was done using an oil-immersion 100× objective. The measuring system fitted with it has 1-μm resolution along the X- and Y-axes and 0.5-μm

resolution along the *Z*-axis. The details of the emulsion plates, their exposure, and other details are given in the Table 1.

The events were chosen utilizing the following criteria:

1. The beam track must be $<3^0$ to the main beam direction in the film. It is done to ensure that we have taken the real projectile beam.
2. The interactions should not be within the top or bottom 20-μm thickness of the film. This is done to reduce the loss of tracks as well as to reduce the error in angle measurement.
3. The track of the incident particle, which induces interaction, is followed back up to the entrance edge of the emulsion plates (marked by arrow). If the track is found to remain parallel to the other noninteracting incident beam tracks, we infer that the event chosen is a primary interaction.

If any interaction is observed to be originated from a non-primary beam, the corresponding event is removed from the sample.

According to the emulsion terminology, the particles emitted after interactions are classified as follows:

1. Black particles: They are target fragments with ionization greater or equal to $10I_0$, where I_0 is the minimum ionization of a single charged particle. They consist of both single and multiple charged fragments, which are smaller than 3 mm in emulsion medium and have velocities smaller than 0.3 c (c is the velocity of light in vacuum).
2. Grey particles: They are mainly fast target recoil protons with energy up to 400 MeV. They have ionization $1.4\ I_0 \leq I < 10I_0$. Their ranges are greater than 3 mm and are having velocities $0.7\ c \geq V \geq 0.3\ c$.
3. Shower particles: The relativistic shower tracks with ionization $I \leq 1.4I_0$ are mainly produced by pions and are not generally confined within the emulsion film. These shower particles have energies in the GeV range. Details of the measurement can be found in Ref. [18].

For the present investigation, 250 events of ^{16}O-AgBr interactions at 60 AGeV were selected.

3 Methodology for Separation of Ring-Like and Jet-Like Substructures

The ring-like and jet-like substructures have been separated using a method described in [36], where we start with a fixed number n_d of particles (shower tracks). Each n_d-tuple of particles put consecutively along the η-axis and can then be considered as a subgroup characterized as follows:

a) Size $\Delta\eta_c = \eta_{max} - \eta_{min}$, where η_{min} and η_{max} are the minimum and maximum values of the pseudo-rapidity in the subgroup.
b) A density $\rho_c = n_d/\Delta\eta_c$.

Thus, each subgroup of particles, dense or dilute, has the same multiplicity and hence can be easily compared with each other. The azimuthal structure of a particular subgroup can now be parametrized in terms of the following quantities,

$$S_1 = -\sum \ln(\Delta\Phi_i)$$
$$\text{and} \quad S_2 = \sum (\Delta\Phi_i)^2$$

where, $\Delta\Phi_i$ is the azimuthal difference between two neighboring particles in the group. For the sake of simplicity, we can count $\Delta\Phi$ in units of full revolutions, and thus, we have

$$\sum (\Delta\Phi_i) = 1$$

Both these parameters will be large ($S_1 \to \infty, S_2 \to 1$) for jet-like structures and small ($S_1 \to n_d \ln n_d$, $S_2 \to 1/n_d$) for ring-like structures.

In the present investigation, we separate ring-like and jet-like substructures with the help of the parameter S_2. Figure 2 shows the $S_2/\langle S_2\rangle$ distribution for our data of ^{16}O–AgBr interactions at 60 AGeV. The distribution shows a peak at $S_2/\langle S_2\rangle = 0.65$. We consider ring-like structured events having $\frac{S_2}{\langle S_2\rangle} < 1$ (0.3–0.7), the rest (0.85–1.65) as jet-like structured events. The detail of separation of ring-like and jet-like events is given in our earlier publications [37–42].

4 Method of Analysis

4.1 G-Moment Method

Hwa and others [32–35] proposed the G_q moment approach, which has enriched study of multifractal analysis in multiparticle production. If the particle production process is self similar in nature, the G_q moments show a remarkable power law behavior. The power law behavior of G_q moment is analyzed event by event and not for the event average, which suppresses the importance of fluctuations in low multiplicity

Table 1 Exposure details of ^{16}O-AgBr interactions at 60 AGeV

Incident beam	Energy	Place of exposure	Type of emulsion	Dimensions	Flux of incident particles
^{16}O	60 AGeV	CERN SPS Switzerland	Illford G5	$18\times7\times0.06$ cm^3	1×10^3 ions per cm^2

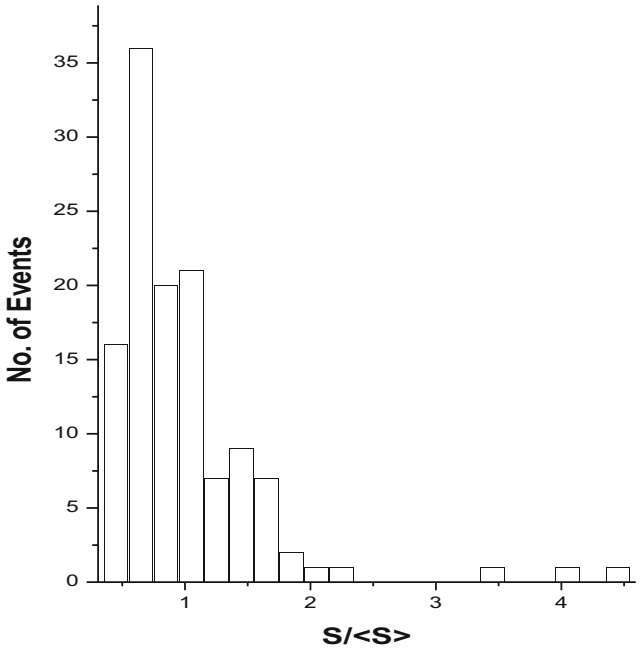

Fig. 2 $S_2/<S_2>$ distribution for pion data of ^{16}O-AgBr interactions at 60 AGeV

events. It is to be mentioned that for low multiplicity events, the fractal moment G_q are dominated by statistical fluctuations. In order to suppress the statistical contribution, a modified form of G_q moments in terms of a step function was suggested by Hwa and Pan [14], which can act as a filter for the low multiplicity events. This method has been used to understand the multifractality in lepton, hadron, and nuclear collisions.

The selected phase space (η and ϕ space) interval of length Δx has been divided into M bins of equal size; the width of each bin is $\delta x = \Delta x/M$. Let n be the total multiplicity of shower particles in the considered phase space interval. Let n_m be the multiplicity of the particles distributed in the mth bin. When M is large, some bins have no particles (empty bins).

Let M be the number of nonempty bins which constitute a set of bins that have fractal properties. Hwa proposed a new set of fractal moments, G_q, defined as:

$$G_q = \sum p_m^q \tag{1}$$

where $p_m = n_m/n$ with $n = \sum n_m$ and q is the order number. Only nonempty bins are taken for the summation to be carried out such that q can cover the whole spectrum of real numbers.

In an attempt to circumvent the problem of statistical noise, Hwa and Pan [14] proposed a modified definition of G-moment, which is,

$$G_q = \sum p_m^q \Theta(n_m - q) \tag{2}$$

where $\Theta\,(n_m - \mathrm{q}) = 1$ is the usual step function which has been added in order to minimize or cut off the statistical noise. It is defined as,

$$\begin{aligned} \Theta(n_m - q) &= 1 \quad \text{if} \quad n_m \geq q \\ &= 0 \quad \text{if} \quad n_m < q \end{aligned}$$

When the multiplicity is very large, i.e., $n/M >> q$, the step function becomes unity and as a consequence, the two definitions coincide. But when n is much less than M, (i.e., the multiplicity is rather low) the function Θ has significant influence on the G moments. Thus, in the real environment of high-energy collisions, the G moments are dominated by statistical fluctuations.

For an ensemble of events, the averaging is done as follows:

$$< G_q >= (1/\Omega) \sum G_q \tag{3}$$

where, Ω is the total no. of events in the ensemble.

From theory of multifractals, a self-similar particle production is characterized by a power law behavior [32, 33]:

$$< G_q >= M^{-\tau_q}$$

where τ_q is the fractal index and can be obtained from the slope of ln $<G_q(M)>$ vs. ln M plot.

$$\tau_q = \delta \ln < G_q(M) > / \delta \ln(M) \tag{4}$$

The dynamical component of $<G_q>$ can be estimated from the formula given by Chiu [16]

$$< G_q >^{\mathrm{dyn}} = \left[< G_q > / < G_q^{\mathrm{st}} > \right] M^{1-q} \tag{5}$$

This gives,

$$\tau_q^{\mathrm{dyn}} = \tau_q - \tau_q^{\mathrm{st}} + q - 1 \tag{6}$$

and generalized fractal dimension

$$D_q^{\mathrm{dyn}} = \tau_q^{\mathrm{dyn}} \Big/ (q-1) \tag{7}$$

The anomalous fractal dimension d_q is defined as

$$d_q = 1 - D_q^{\mathrm{dyn}}$$

If G_q is purely statistical, then $<G_q>^{\mathrm{dyn}} = M^{1-q}$ which is the result of trivial dynamics. Under such a condition, $\tau_q^{\mathrm{dyn}} = q - 1$. Any deviation of τ_q^{dyn} from $q-1$ indicates the presence of dynamical information.

4.2 Factorial Moment Method

Let the phase space interval ΔX be divided into M bins of size $\delta X=\Delta X/M$. The normalized factorial moment F_q of order q is defined as [9]

$$F_q(\delta X) = M^{q-1}\sum_{m=1}^{M} \frac{n_m(n_m-1).....(n_m-q+1)}{\langle n_m\rangle^q} \tag{8}$$

where, n_m is the multiplicity in the mth bin, $\langle..\rangle$ indicates average over the whole sample of events. For given q and M values, F_q's are calculated for all the events and then averaged over the whole sample of events to obtain $<F_q>$. The most outstanding feature of this moment is that it can detect and characterize the nonstatistical density fluctuations in particle spectra, which are intimately connected with the dynamics of particle production. Another significant aspect about F_q is that an event can contribute to (8) only if $n_m \geq q$. Thus, for small δX where $\langle n_m\rangle$ is small in a bin, only rare events with high spikes ($n_m \geq q$) contribute.

At the critical point when hadrons are produced, one expects the spatial pattern of the produced particles in phase space to exhibit self-similar behavior, which ideally (as in the Ising model [31]) would imply a power-law dependence of F_q on M, that is in the limit of small bin size.

$$\begin{aligned} &< F_q > \propto M^{\alpha_q} \\ \text{i.e.,}\quad &\ln < F_q >= \alpha_q \ln M + e \end{aligned} \tag{9}$$

This property, in analogy with turbulent fluid dynamics, is called "intermittency." α_q measures the strength of the intermittency and is called the intermittency exponent, and e is a constant. The intermittency exponent α_q is obtained by performing best fits according to Eq. (9).

We have established a relation between the fractal codimensions (d_q) and intermittency indices (α_q)

$$d_q = \frac{\alpha_q}{(q-1)} = 1-D_q \tag{10}$$

where d_q is the anomalous fractal dimension or Renyi codimension and measures the intermittency dimension. D_q is the generalized qth order Renyi dimension which describes fractal and multifractal in the classical system. The monofractal structure of multiparticle spectra will show order-independent intermittency indices, whereas in the case of multifractality, $D_q<D_{q'}$ for $q>q'$.

4.3 Multifractal Specific Heat

It is well known that in usual thermodynamics, in many important cases, the specific heat of gases and solids is constant, independent of temperature, over a greater or smaller temperature interval [43] which is also known as constant heat approximation (CSH). This approximation is also applicable to multifractal data of multiparticle production process. This has been shown by Bershadkii [25]. If the q dependence of D_q^{dyn} satisfies the condition $D_q>D_{q'}$ for $q<q'$, then the spectra is said to exhibit multifractality and the corresponding multifractal specific heat can be obtained from generalized dimension D_q^{dyn} by the following relation if the thermodynamical interpretation of multifractality is used [25, 44].

$$D_q = (a-c) + c\frac{\ln q}{q-1} \tag{11}$$

Here c *i*s the specific heat and a is a constant. The multifractality-monofractality phase transition corresponds to a gap from $c=0$ to a finite nonzero value of c. Hence, the study of c is quite significant as it allows us to consider this transition (multifractality-monofractality) as a thermodynamic phase transition [43] in high-energy nuclear collisions.

4.4 Levy Index Analysis

The Levy stable laws were introduced by Brax and Peschanski [29] to describe intermittency in multiparticle production process. For the analysis, a generalization of the central theorem limit was applied to random cascading models. The resultant was a one-parameter family of representative models depending continuously on the Levy index μ.

Brax and Peschanski [29] argued that Gaussian approximation is often inaccurate particularly for higher order of moments, and hence used Levy laws.

The Levy stable law is characterized by the Levy stability index μ, which is considered to be a measure of the degree of multifractality. Corresponding to the physically allowed limit μ lies between 0 and 2. Under the Levy law approximation [29], the ratio of anomalous dimensions is expected to follow a relation, like

$$\frac{d_q}{d_2}(q-1) = \beta_q = \frac{(q^\mu - q)}{(2^\mu - 2)} \tag{12}$$

The index μ, as discussed previously, allows an estimation of the cascading rate [29] and also indicates the fractality. The Levy stable law was able to explain multiplicity fluctuations or intermittency quite well, as well as speculate the formation of QGP in high-energy interactions [28, 45].

5 Results and Discussions

We have performed all the studies in one-dimensional pseudo-rapidity space (η) and azimuthal angle space (ϕ). Where η, the pseudo-rapidity is defined in terms of emission angle (θ) as $\eta=-\ln\tan\theta/2$. As the shape of this distribution influences the scaling behavior of the factorial moments, we have used the

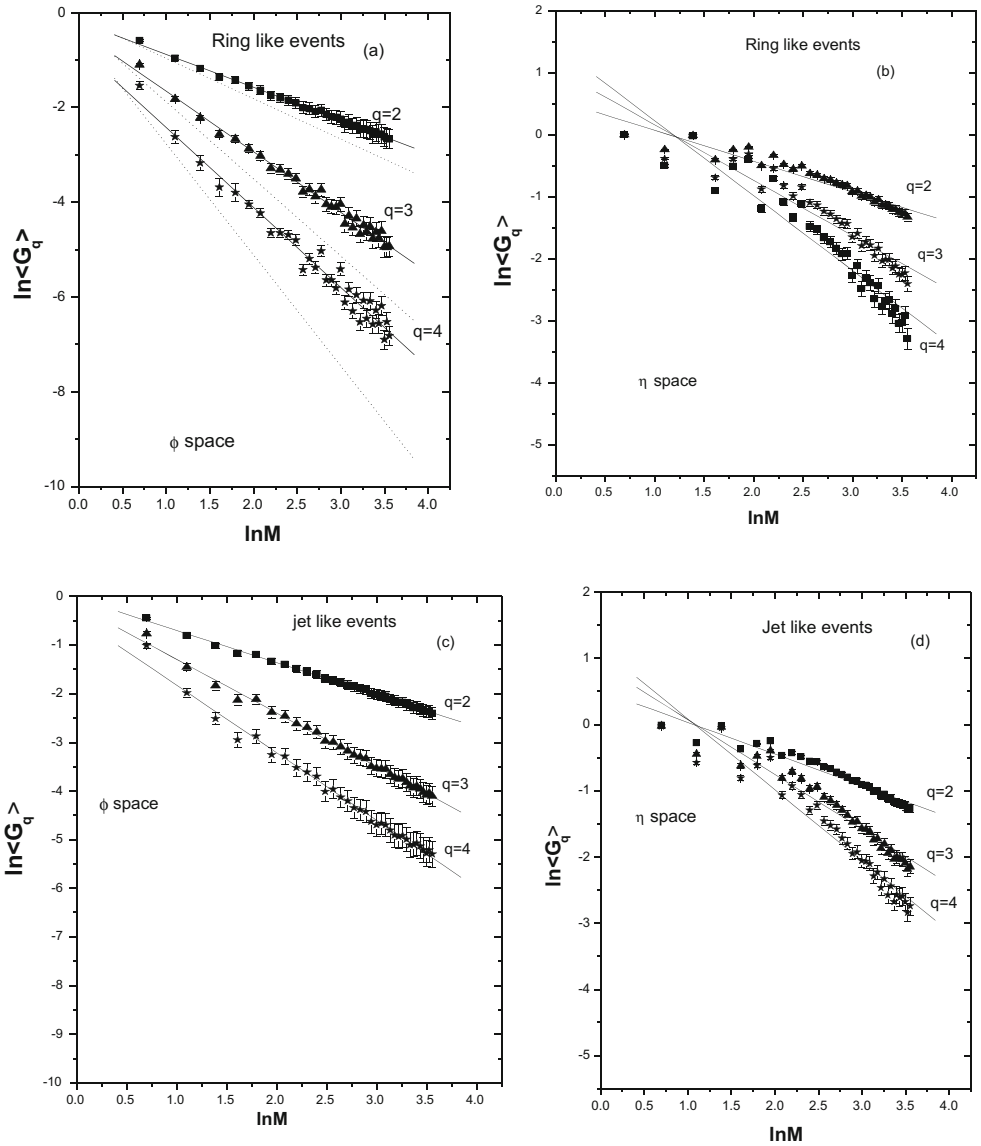

Fig. 3 $\ln<G_q>$ vs lnM for ring-like events in **a** ϕ space, **b** η space and for jet-like events in **c** ϕ space, **d** η space

Table 2 Values of D_q^{dyn} in η-space and ϕ-space for ring-like and jet-like events for G_q moment analysis

Type of substructure	Phase space	q	τ_q	τ_q^{st}	τ_q^{dyn}	D_q^{dyn}
Ring-like	η	2	0.497±0.025	0.621±0.030	0.876±0.039	0.876±0.039
		3	0.896±0.048	1.184±0.063	1.712±0.079	0.856±0.040
		4	1.208±0.066	1.714±0.096	2.494±0.116	0.831±0.039
Jet-like	η	2	0.477±0.022	0.65±0.027	0.827±0.035	0.827±0.035
		3	0.826±0.038	1.23±0.057	1.596±0.069	0.798±0.034
		4	1.069±0.048	1.77±0.085	2.299±0.097	0.766±0.033
Ring-like	ϕ	2	0.696±0.007	0.851±0.005	0.845±0.009	0.845±0.009
		3	1.277±0.024	1.627±0.012	1.650±0.027	0.825±0.014
		4	1.688±0.050	2.343±0.021	2.345±0.054	0.782±0.018
Jet-like	ϕ	2	0.659±0.006	0.817±0.004	0.842±0.007	0.842±0.007
		3	1.102±0.013	1.57±0.010	1.532±0.016	0.766±0.008
		4	1.386±0.025	2.276±0.017	2.11±0.030	0.703±0.010

"cumulative" variable X_η instead of η. The corresponding region of investigation for the variable then become (0, 1). The cumulative variable X_η is given by the following relation [46]:

$$X_\eta = \frac{\int_{\eta_{\min}}^{\eta} \rho(\eta)d\eta}{\int_{\eta_{\min}}^{\eta_{\max}} \rho(\eta)d\eta}$$

where $\eta_{\min}$ and $\eta_{\max}$ are two extreme points in the distribution $\rho(\eta)$, between which X_η varies from 0 to 1. Due to the scale properties of the variables, the one-particle spectrum stretches in its central region, eliminating the losses from the beam splitting and thus allowing to observe the higher order of moments. A similar approach has been adopted for the analysis in azimuthal phase space. The "cumulative" variable X_φ instead of ϕ is used in the analysis, such that X_φ varies from 0 to 1, when ϕ varies from 0 to 2π.

5.1 G_q Moment Analysis

We have analyzed the pionisation data obtained from ^{16}O-AgBr interactions at 60 AGeV for both ring-like and jet-like events in one-dimensional pseudorapidity (η) and azimuthal angle space (ϕ). We have divided both X_φ space and X_η space into M=2, 3, 4….. 35 bins for both ring-like and jet-like events. For each event, we have calculated the G moments for orders 2, 3, 4 using Eq. (2). The event averaged G moments of order q=2,3,4 has been plotted against lnM in Fig. 3a, b, respectively, in ϕ space and η space for ring-like

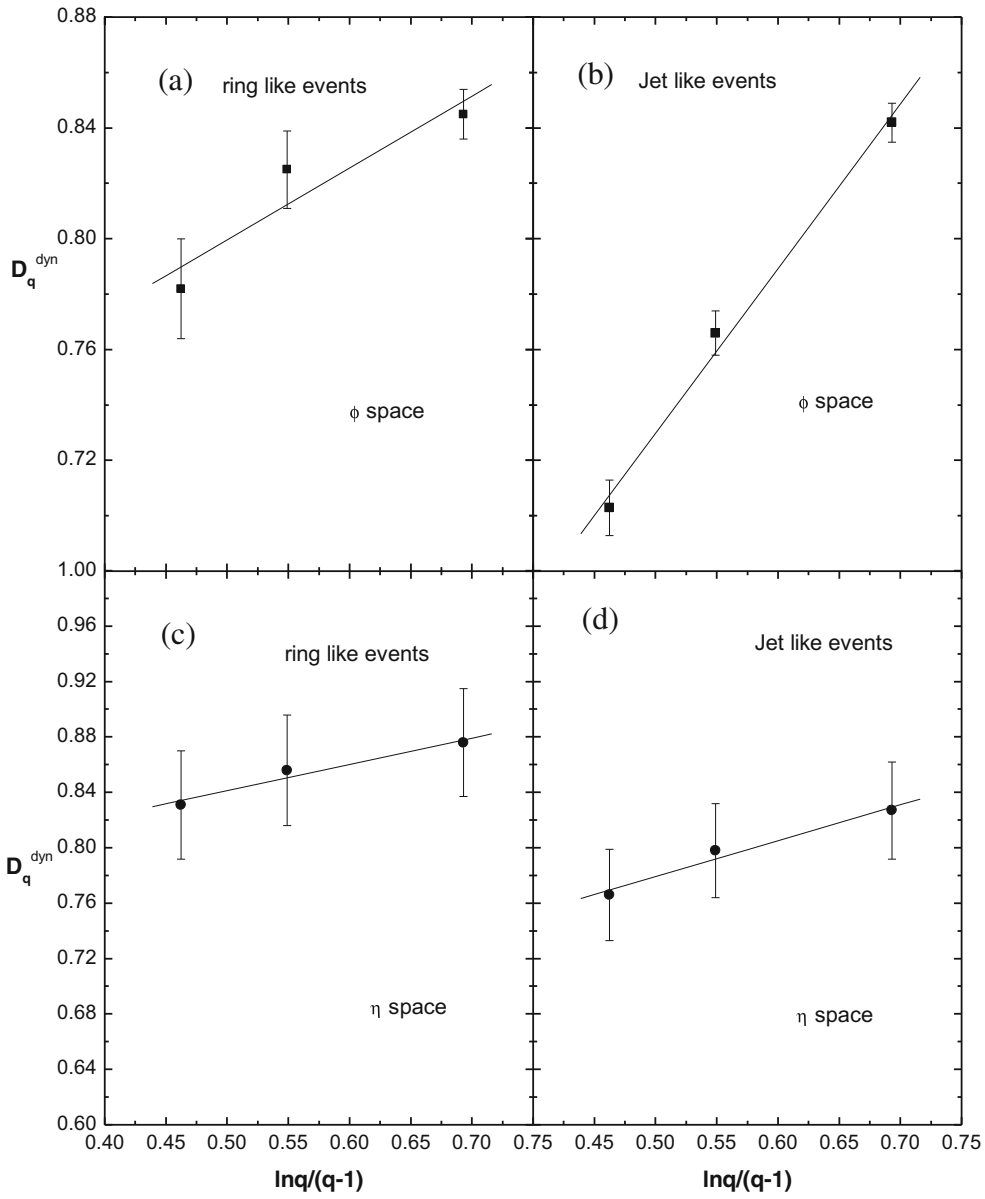

Fig. 4 D_q vs lnq/(q−1) graph in ϕ space for **a** ring-like events, **b** jet-like events and in η space for **c** ring-like events, **d** jet-like events for G_q moment analysis

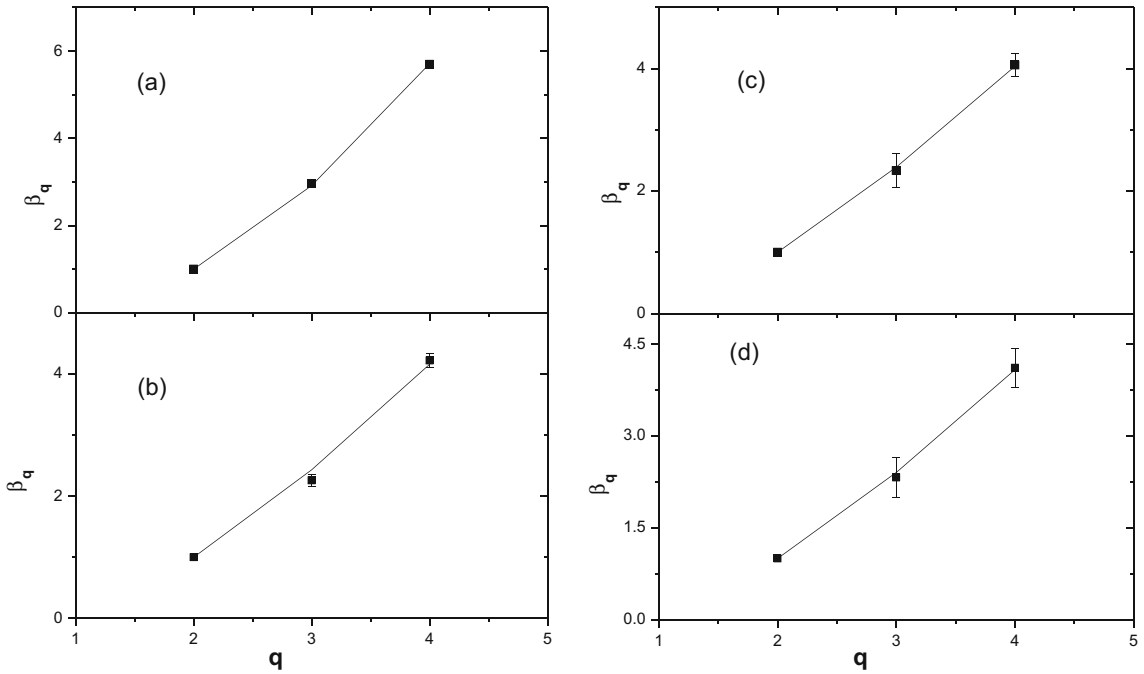

Fig. 5 β_q vs q graph in ϕ space for **a** jet-like events, **b** ring-like events and in η space for **c** jet-like events, **d** ring-like events for G_q moment analysis

events and in Fig. 3c, d, respectively, in ϕ space and η space for jet-like events. A linear dependence of ln$<G_q>$ and lnM is observed, indicating self-similarity in the particle emission process. The exponent τ_q is obtained by least square fitting of the data points. The values are listed in Table 2 for ring-like and jet-like events in the η and ϕ spaces, respectively.

To estimate the statistical contribution to $<G_q>$, we distribute the n particles of an event randomly in the specific x interval, and using the same procedure, we calculate $<G_q^{st}>$

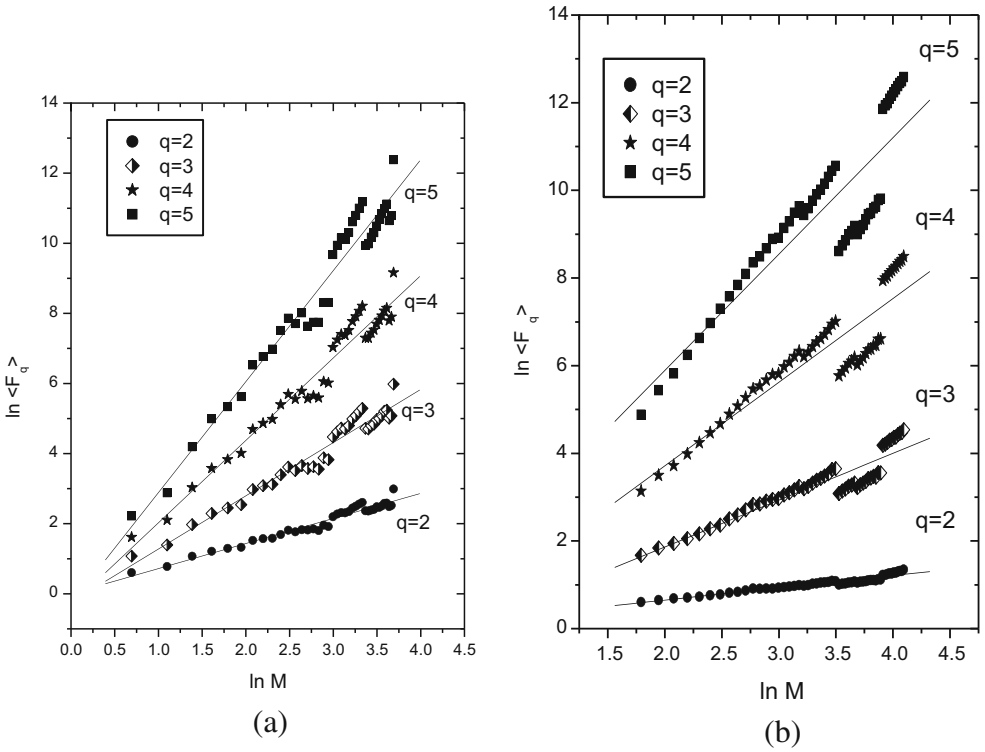

Fig. 6 lnM vs. ln$<F_q>$ in η space for **a** ring-like and **b** jet-like events

as in Eq. (3) and τ_q^{st} as in Eq. (4). The best fitted lines for ln $<G_q^{st}>$ vs ln M plot are shown by dotted lines in Fig. 3a–d, correspondingly, with the experimental data. The slopes τ_q^{st} are listed in Table 2 correspondingly. The values of τ_q^{dyn} and D_q^{dyn} for ring-like and jet-like events in both ϕ space and η space have been calculated using Eqs. (6) and (7), respectively, and tabulated in Table 2. From our analysis, it is evident that D_q^{dyn} decreases with q, the order of the moments for ring-like and jet-like events in both ϕ space and η space showing multifractal nature and self-similarity in relativistic multiparticle production processes.

The values of generalized dimension D_q^{dyn} for both ring-like and jet-like events are plotted against $\ln q/(q-1)$, respectively, in Fig. 4a, b in ϕ space and Fig. 4c, d in η space to extract the multifractal specific heat using Eq. (11). The linear behavior in Fig. 4a, b indicates that the slope (value of multifractal specific heat) is more for jet-like events for ring-like events in ϕ space. The values of multifractal specific heat c are tabulated in Table 4. We note from Table 4 that the values of c are smaller for ring-like events in both ϕ space and η space for jet-like events.

We have calculated β_q using Eq. (12) for both jet-like and ring-like events and plotted with respect to q, respectively, in Fig. 5a, b in ϕ space and Fig. 5c, d in η space and determined the values of μ from the plots. The values of μ are tabulated in Table 5. It is seen from Table 5 that values of μ for ring-like events are different from that of jet-like events in both phase spaces, which indicates different degree of multifractality. However, in all the cases, the values of μ are within the limit $1 \leq \mu \leq 2$, which indicates a nonthermal phase transition in the cascading process.

5.2 Factorial Moment Analysis

We have studied the M dependence of $<F_q>$ against in a log-log plot of different orders q (q=2, 3, 4, 5) for both (ring and jet) types of events in one-dimensional η space for ^{16}O-AgBr interaction at 60 AGeV. We have divided the X_η space into M=2, 3, 4….. 35 bins for both ring-like and jet-like events. For each event, we have calculated the F_q moments for orders 2, 3, 4, 5 using Eq. (8). The values of ln$<F_q>$ vs lnM are plotted in Fig. 6a for ring-like event and in Fig. 6b for jet-like events in η space, respectively. From Fig. 6a, b, it can be seen that the ln$<F_q>$ vs lnM plot exhibits linearity for all values of q in η space for ring-like and jet-like events as expected from Eq. (9). Similar observations were made for the ϕ space and can be obtained from [47]. This indicates self-similarity in the particle emission process and existence of fractal properties. Table 3 shows the values of the intermittency indices α_q as obtained from Eq. (9) and the values of anomalous fractal dimension d_q and generalized fractal dimension D_q as obtained from Eq. (10) in η space for ring-like and jet-like events, respectively. Table 3 also shows the values of the intermittency indices α_q obtained from [47] and the values of anomalous fractal dimension d_q and generalized fractal dimension D_q as obtained from Eq. (10) in ϕ space for ring-like and jet-like events, respectively. From Table 3, it is clear that the values of the generalized fractal dimension D_q decrease with increasing order of moment, which is a clear indication of multifractality.

In Fig. 7a–d, D_q is plotted as a function of $\ln q/(q-1)$ for both ring-like and jet-like events in ϕ space and η

Table 3 Values of D_q^{dyn} in η-space and ϕ-space for ring-like and jet-like events for F_q moment analysis

Phase space	Type of substructure	q	α_q	d_q	D_q
η	Ring-like	2	0.716±0.025	0.716±0.025	0.284±0.025
		3	1.518±0.055	0.759±0.028	0.241±0.028
		4	2.351±0.083	0.784±0.028	0.216±0.028
		5	3.167±0.110	0.792±0.027	0.208±0.027
	Jet-like	2	0.280±0.102	0.280±0.102	0.720±0.102
		3	1.068±0.059	0.534±0.030	0.466±0.030
		4	1.909±0.125	0.636±0.042	0.364±0.042
		5	2.655±0.194	0.664±0.049	0.336±0.049
ϕ	Ring-like	q	α_q[47]	d_q	D_q
		2	0.141±0.004	0.141±0.004	0.859±0.004
		3	0.437±0.015	0.218±0.008	0.781±0.008
		4	0.830±0.038	0.277±0.013	0.723±0.013
		5	1.226±0.069	0.306±0.017	0.693±0.017
	Jet-like	2	0.180±0.005	0.180±0.005	0.820±0.005
		3	0.568±0.022	0.284±0.011	0.716±0.011
		4	1.106±0.050	0.369±0.017	0.631±0.017
		5	1.674±0.085	0.418±0.021	0.582±0.021

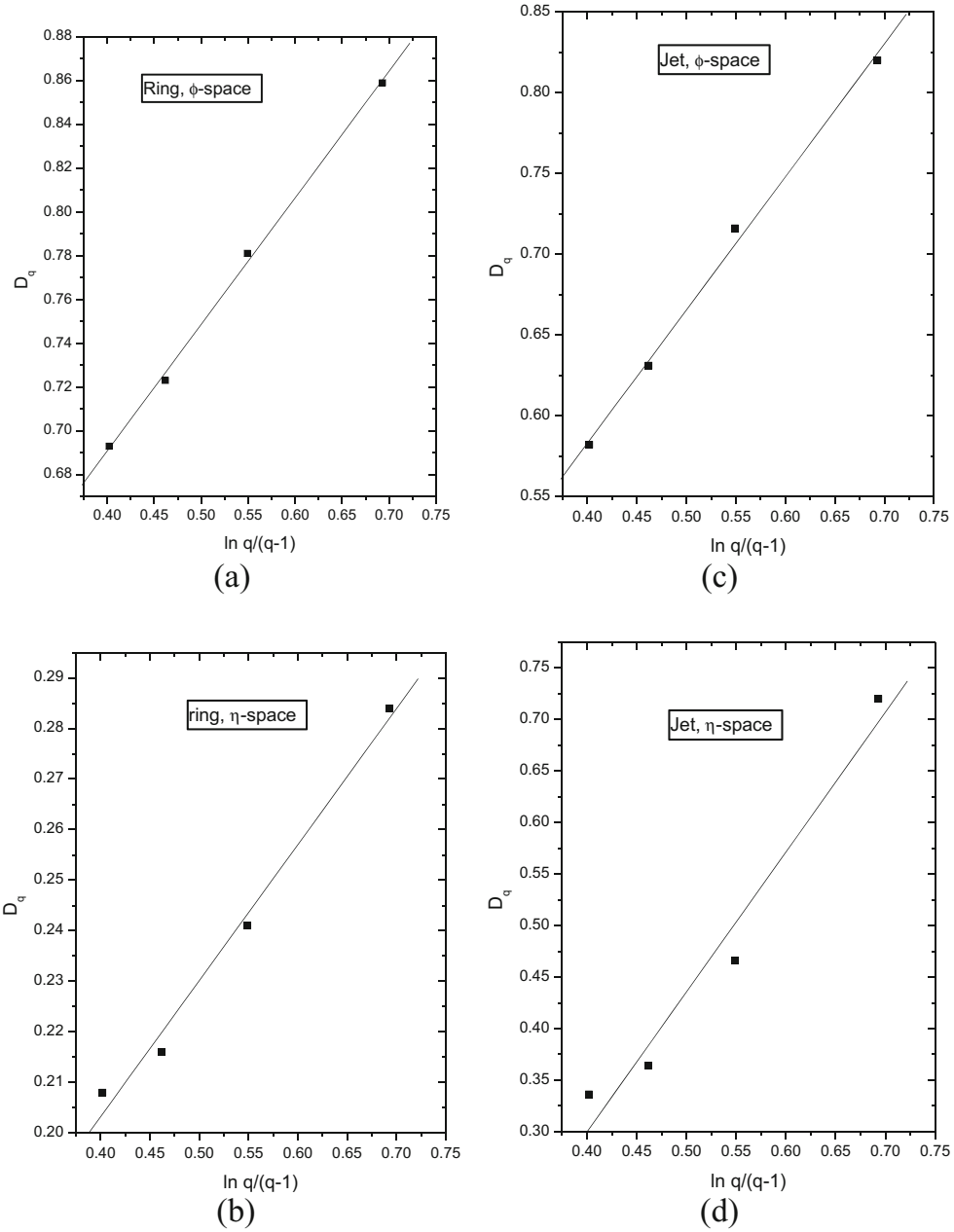

Fig. 7 D_q vs lnq/(q−1) for ringlike events **a** in ϕ space and **b** in η space and for jet-like events **c** in ϕ space and **d** in η space for F_q moment analysis

space, from which the values of multifractal specific heat is calculated using Eq. (11) and tabulated in Table 4. It can be seen from Table 4 that the values of multifractal specific heat c is larger for jet-like events

Table 4 Multifractal specific heat in ϕ-space and in η-space for ring-like and jet-like events for both G_q moment and F_q moment analysis

Type of substructure	Phase space variable	Multifractal specific heat (c)	
		G_q moment method	F_q moment method
Jet-like	ϕ	0.594±0.052	0.82±0.04
		0.258±0.044	1.36±0.19
Ring-like	ϕ	0.259±0.094	0.58±0.02
	η	0.189±0.039	0.27±0.02

Table 5 Levy indices in ϕ-space and in η-space for ring-like and jet-like events for both G_q moment and F_q moment analysis

Type of substructure	Phase space variable	Values of Levy index μ	
		G_q moment method	F_q moment method
Jet-like	ϕ	1.891±0.012	1.915±0.043
	η	1.027±0.027	1.993±0.105
Ring-like	ϕ	1.111±0.017	1.808±0.049
	η	1.059±0.041	0.332±0.012

as compared to ring-like events of the corresponding phase space (η or ϕ).

The Levy index values for ring-like and jet-like events in η and ϕ phase space are calculated using Eq. (12). The values of β_q for the above-mentioned cases are shown in Table 5, β_q is plotted as a function of q defined by Eq. (12), from which the values of the Levy index μ were determined. The plots are shown in Fig. 8a–d for ring-like and jet-like events (for both ϕ space and η space). The results so obtained are given in Table 5.

It is to be mentioned that for all the above analysis, the errors in all the figures and tables are only from the diagonal terms of the covariance error matrix. However, it is observed that the diagonal terms provide the main contributions and the non-diagonal terms that account for the correlation between different bin sizes do not contribute appreciably [48].

6 Conclusions

To shed light on the nature of pion emission process for both ring-like events and jet-like events, we have calculated the dynamical component of generalized dimension D_q^{dyn} using Eq. (7) and tabulated in Table 2 for G_q moment method. It is evident from the variation of D_q^{dyn} with the order q that the pion emission process is multifractal in nature for ring-like events as well as jet-like events in both pseudorapidity space and azimuthal

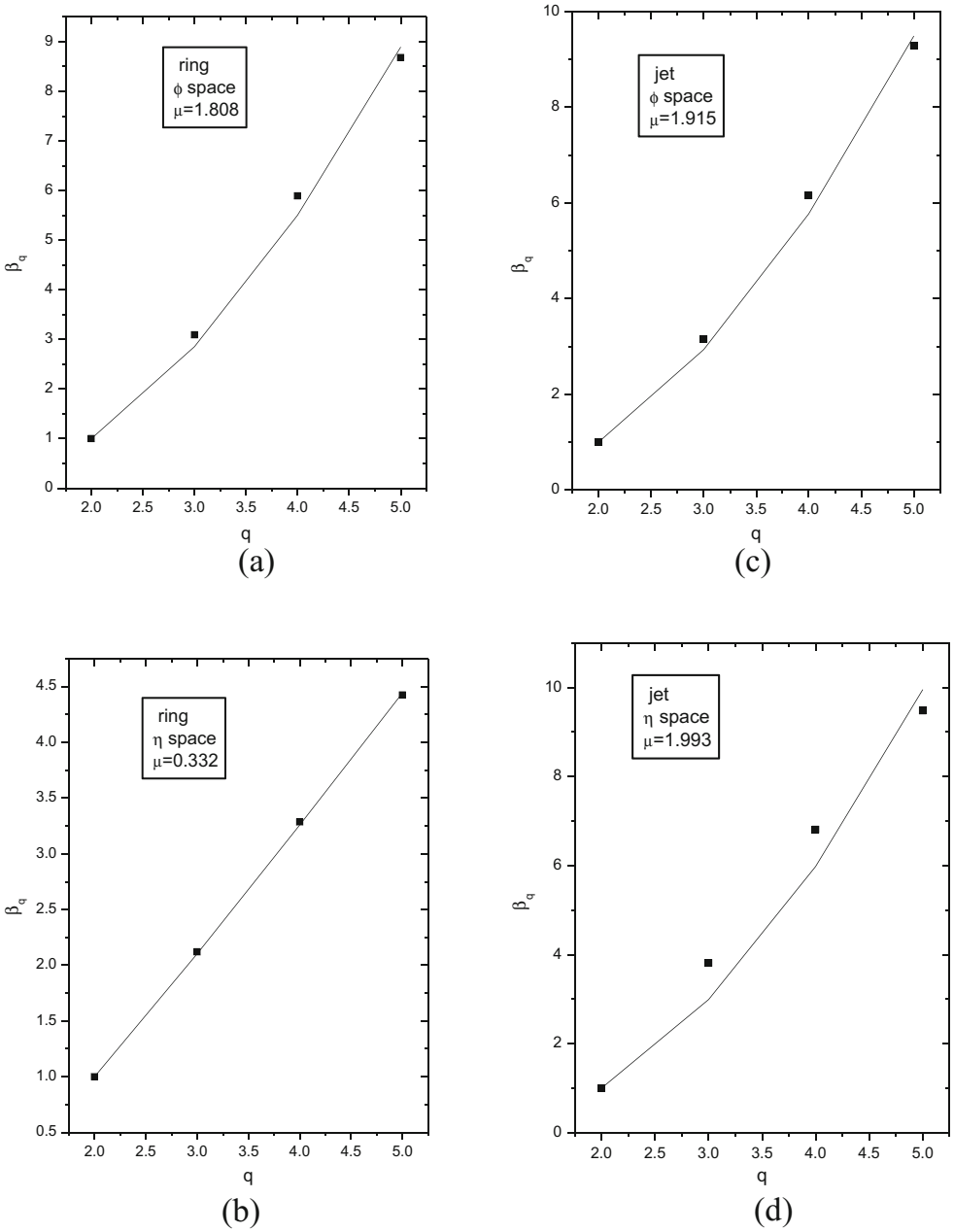

Fig. 8 β_q vs q for ring-like events **a** in ϕ space and **b** in η space and for jet-like events **c** in ϕ space and **d** in η space for F_q moment analysis

angle space. However, comparing with F_q moment analysis (Table 3), it is seen that D_q (calculated using Eq. (10)) decrease with increasing order of the moment, which is a clear indication of multifractality. Therefore, we can conclude that multifractality occurs in η and ϕ phase space for ring-like and jet-like events using G_q moment and F_q moment analysis.

Using the thermodynamical interpretation of multifractality [25, 44], we have extracted the multifractal specific heat c [Eq. (12)] for ring-like events as well as for jet-like events in both phase spaces and tabulated in Table 4 for both G_q moment method and F_q moment method. It is observed from Table 4 that the values of "c" are less in case of ring-like events in both ϕ space and η space than that of jet-like events for G_q moment analysis. However, there is no uniformity in the values of c in ring-like and jet-like events observed for F_q moment analysis.

The values of multifractal specific heat calculated using G_q moment method and F_q moment method are different from each other, which may be consequence of the fact that the two approaches are different.

To estimate the degree of multifractality as well as the nature of phase transition, the Levy stability index μ [Eq. (12)] has been determined for each of the data sets and tabulated in Table 5 for both G_q moment method and F_q moment method. The value of Levy indices indicates nonthermal phase transition in the cascading process and different fractal behavior in the pion production process of ring-like events and jet-like events for G_q moment analysis. From Table 5, it is seen that for pions, when F_q moment methodology is applied, the value of μ obtained for ring-like events in η space is around 0.332 (less than 1 but more than 0), which indicates thermal phase transition interspersed in the cascading process. For all the other cases, the values of μ obtained is greater than 1(but less than 2) indicating nonthermal phase transition during the cascading process.

Acknowledgments The authors are grateful to Prof. P.L. Jain (Buffalo State University, USA) for providing the emulsion plate exposed to ^{16}O beam. The authors are also grateful to the reviewers for their valuable comments and suggestions.

References

1. R Peschanski, *XXII Int. Symp. On Multiparticle Dynamics* (1992)
2. A.V. Apanasenko, N.A. Dobrotin, I.M. Dremin, K.A. Kotelnikov, JETP Lett. **30**, 157 (1979)
3. I.M. Dremin, JETP Lett. **30**, 145 (1979)
4. I.M. Dremin, A.M. Orlov, M.I. Tret'yakova, JETP Lett. **40**, 1115 (1984)
5. I.M. Dremin, L.I. Sarycheva, K.Y. Teplov, Eur. Phys. J. C **46**, 429 (2006)
6. M. Spouta, Indian J. Phys. **85**, 1063 (2011)
7. I.M. Dremin, Nucl. Phys. A **767**, 233 (2006)
8. A.E. Glassgold, W. Heckrotte, K.M. Watson, Ann. Phys. **6**, 1 (1959)
9. A. Bialas, R. Peschanski, Nucl. Phys. B **273**, 703 (1986)
10. A. Bialas, R. Peschanski, Nucl. Phys. B **308**, 857 (1988)
11. W. Ochs, J. Wosiek, Phys. Lett. B **214**, 617 (1988)
12. L. Van Hove, Ann. Phys. **192**, 66 (1989)
13. B. Mendelbrot, J. Fluid Mech. **62**, 331 (1974)
14. R.C. Hwa, J.C. Pan, Phys. Rev. D **45**, 1476 (1992)
15. C.B. Chiu, R.C. Hwa, Phys. Rev. D **45**, 2276 (1989)
16. C.B. Chiu, K. Fialkowski, R.C. Hwa, Mod. Phys. Lett. A **5**, 2651 (1990)
17. D. Ghosh et al., Mod. Phys. Lett. B **5**, 272 (1991)
18. D. Ghosh, A. Deb, P.K. Halder, S.R. Sahoo Md, A.K. Jafry, Nucl. Phys. A **707**, 213 (2002)
19. P.L. Jain et al., Phys. Rev. C **46**, 721 (1992)
20. E.A. De Wolf, I.M. Dremin, W. Kittel, Phys. Rep. **270**, 48 (1996)
21. R. Peschanski, Int. J. Mod. Phys. A **6**, 3681 (1991)
22. A. Arneodo, E. Bacry, J.F. Muzy, Physica A **213**, 232 (1995)
23. H. Satz, Nucl. Phys. B **326**, 613 (1989)
24. R.C. Hwa, M.T. Nazirov, Phys. Rev. Lett. **65**, 741 (1992)
25. A. Bershadskii, Eur. Phys. J. A **2**, 223 (1998)
26. G. Paladin, A. Vulpiani, Phys. Rep. **156**, 147 (1987)
27. A. Bershadkii, Phys. Rev. C **59**, 364 (1999)
28. A. Bialas, R.C. Hwa, Phys. Lett. B **253**, 436 (1991)
29. P. Brax, R. Peschanski, Phys. Lett. B **253**, 225 (1991)
30. S. Hegyi, Phys. Lett. B **318**, 642 (1993)
31. J. Wosiek, Acta Phys. Polon. B **19**, 863 (1988)
32. R.C. Hwa, Phys. Rev. D **41**, 1456 (1990)
33. C.B. Chiu, R.C. Hwa, Phys. Rev. D **43**, 100 (1991)
34. W. Florkowski, H.C. Hwa, Phys. Rev. D **43**, 1548 (1991)
35. H.G.E. Hentschel, I. Procaccia, Physica D **8**, 435 (1983)
36. M. Adamovich et al., J. Phys. G **19**, 2035 (1993)
37. P.K. Halder, S.K. Manna, P. Saha, D. Ghosh, Pramana **80**, 631 (2013)
38. D. Ghosh, A. Deb, P.K. Halder, S. GuptaRoy, Astropart. Phys. **27**, 127 (2007)
39. D. Ghosh, A. Deb, P.K. Halder, A. Dhar (Mitra), Europhys. Lett. **80**(22003) (2007)
40. D. Ghosh, A. Deb, A. Dhar (Mitra), P.K. Halder, Acta Phys. Pol. B **40**, 1001 (2009)
41. P.K. Halder, S.K. Manna, Chin. Phys. Lett. **28**, 012502 (2011)
42. P.K. Halder, S.K. Manna, Can. J. Phys. **89**, 713 (2011)
43. L.D. Landau, E.M. Litshitz, *Statistical Physics Pergamon*, 1980
44. E. Stanley, P. Meakin, Nature **355**, 405 (1988)
45. W. Ochs, Z. Phys. C **50**, 339 (1991)
46. A. Bialas, M. Gazdzicki, Phys. Lett. B **252**, 483 (1990)
47. D. Ghosh et al., Indian J. Phys. **80**, 807 (2006)
48. N.M. Agababyan et al., Phys. Lett. B **382**, 305 (1996)